



ELSEVIER

Journal of Chromatography A, 830 (1999) 29–39

JOURNAL OF  
CHROMATOGRAPHY A

# Estimation of the column radial heterogeneity from an analysis of the characteristics of tailing peaks in linear chromatography

Kanji Miyabe<sup>a,b</sup>, Georges Guiochon<sup>a,b,\*</sup>

<sup>a</sup>*Department of Chemistry, University of Tennessee, Knoxville, TN, 37996-1600, USA*

<sup>b</sup>*Division of Chemical and Analytical Sciences, Oak Ridge National Laboratory, Oak Ridge, TN 37831, USA*

Received 5 August 1998; received in revised form 19 October 1998; accepted 19 October 1998

## Abstract

An estimation procedure of the radial heterogeneity of the distributions of the mobile phase flow velocity and of the local column efficiency was derived from a comparison of experimental data and of the characteristics of these tailing peaks calculated numerically. The analysis of these characteristics indicated that the radial heterogeneity of the packing density of a column is a cause of peak tailing. This analysis showed also that it is possible to correlate the radial fluctuations of the flow velocity and the apparent efficiency of different columns. The comparison of experimental data and calculated results suggested also a correlation between the radial distributions of the flow velocity and of the column efficiency. Previous experimental data concerning the radial heterogeneity of column packings validated the correlation. Information on the degree of heterogeneity of the radial distributions of the flow velocity and the column efficiency were obtained by analyzing the peak width and the asymmetry factor of elution peaks. It was also found that the exponentially modified Gaussian distribution cannot provide a comprehensive representation of all types of tailing profiles in chromatography. © 1999 Elsevier Science B.V. All rights reserved.

**Keywords:** Peak shape; Column radial heterogeneity; Column efficiency; Column packing

## 1. Introduction

It is well known that the columns used in chromatography are not homogeneous [1]. Knox and co-workers were the first to show the radial heterogeneity of the packing of these columns [2,3]. Other studies led to similar conclusions [4–6]. Because these studies showed the existence of two regions in the column, one nearly homogeneous in its center, one more perturbed along its wall, the phenomenon was called the ‘wall effect’ [1,7]. The thickness of the perturbed region of the packing structure near the

column wall was estimated at about 30–50 particle diameters in analytical columns [1,4–6]. However, not enough information was collected to allow any final conclusion.

More systematic studies of the radial distributions of the mobile phase flow velocity, the column local efficiency (height equivalent to a theoretical plate, HETP), and the sample concentration were made recently. They used slurry-packed columns fitted with several on-column, local electrochemical [8] or fluorescence detectors [9–11]. It was found that the flow velocity of the mobile phase was several percent lower in the wall region than in the center of the columns while the HETP was several times

\*Corresponding author.

larger in the wall region than in the center core. The apparent or overall efficiency of the columns depends on the extent of the radial fluctuations of the mobile phase flow velocity and of the local HETP. The radial distributions of the flow velocity and the HETP can be represented by parabolic functions. Similar results have also been obtained from studies of column packing using PFG NMR [12–14]. Finally, Yun and Guiochon made photographs demonstrating that the irregular region affected by the ‘wall effect’ in large diameter columns extends far from the wall, in contrast with the accepted opinion that it extends only over 30–50 particle diameters [15]. Using numerical calculations based on a model including two space coordinates (the column length and its radius), they also showed that peak tailing can arise from column radial heterogeneity [16,17].

Peak tailing brings about unfavorable effects in chromatographic separations, mainly the reduction of the overall column efficiency, hence of the resolution between peaks. The following three causes have been pointed out as instrumental sources of peak tailing, a tailing injection profile, a slow detector response, and a dead volume in some tube connections. However, the influence of these instrumental sources can be reduced by selecting appropriate experimental conditions and by using well-designed instruments. In addition to these sources of tailing, the influence of an heterogeneous mass transfer kinetics on the peak profile becomes important when there are strong, specific interactions between the sample components and the stationary phase, such as in chiral separations or in the analysis of strong bases by RPLC. Guiochon et al. [18] and Fornstedt et al. [19,20] made detailed studies of this influence on the peak tailing by applying a transport-dispersive model. They provided a consistent interpretation to the tailing phenomena in both linear and nonlinear chromatography by assuming the presence of two different sites of adsorption, which have different equilibrium isotherms and different rates of mass transfer kinetics. They proved that the heterogeneous mass-transfer kinetics was an essential source of peak tailing. Peak tailing is also observed in the elution of nonretained tracers and in chromatographic separations of substances capable only of hydrophobic interactions with the stationary phase. Another origin of tailing, other than the sources

listed above, must be found. Previous experimental studies [8–11,16,17] concluded that the radial heterogeneity of the column packing should be considered as this source of peak tailing. In a previous paper [21], we reported the results of a numerical study on the influence of the column heterogeneity on peak tailing.

It is probably impossible to eliminate completely peak tailing due to the local fluctuations of the flow velocity and of the column efficiency because radial heterogeneity is generally present to a degree in all conventional HPLC columns [1]. Therefore, it is necessary to evaluate the degree of column radial heterogeneity and to clarify its influence on peak tailing. The goal of this paper is the derivation of correlations between the radial fluctuations of the flow velocity and of the column efficiency and the extent of tailing of the chromatographic peak profiles. This information was derived by comparing experimental data and the results of calculations regarding the characteristic features of the profiles of tailing peaks.

## 2. Theory

We consider only chromatographic separations under conditions of linear equilibrium isotherm in this study. Unexpectedly tailing peaks are observed in practice under such conditions. The following model was applied to explain this effect. The column was divided into 50 coaxial annular columns. The thickness of each annular column was the same, equal to 1/50 of the column radius. It was also assumed that there was no radial dispersion and that each annular column was homogeneous. The peak profile leaving from each annular column was assumed to be given by the Gaussian function, on the basis of previous experimental data [11].

$$C_d = \frac{1}{\sigma_d \sqrt{2\pi}} \exp\left(-\frac{(1-t_d)^2}{2\sigma_d^2}\right) \quad (1)$$

where  $C_d$  and  $t_d$  are the dimensionless concentration and time, respectively, and represented as follows [18].

$$C_d = \frac{C t_R}{A_p} = \frac{C \epsilon S L (1 + k'_0)}{n} \quad (2)$$

$$t_d = \frac{t}{t_R} = \frac{ut}{L(1+k'_0)} \quad (3)$$

where  $C$  is the actual concentration,  $t_R$  the apical retention time<sup>1</sup>,  $A_p$  the area of the injected pulse,  $\epsilon$  the total porosity of the column,  $S$  and  $L$  the column cross-sectional area and length, respectively,  $k'_0$  the retention factor at infinite dilution,  $n$  the amount of the sample substance injected,  $t$  the time, and  $u$  the interstitial velocity of the mobile phase. The first moment,  $\mu_1$ , and the second central moment,  $\mu_2'$ , of the peak given by Eq. (1) are equal to unity and  $\sigma_d^2$ , respectively. The corresponding number of theoretical plates,  $N$ , is the reciprocal of the dimensionless variance,  $1/\sigma_d^2$ . It was finally assumed that the overall elution peak is obtained as the summation of each Gaussian profile weighed in proportion to the cross-section area of each annular column. The flow velocity,  $u_r$ , and the number of theoretical plates,  $N_r$ , at a radial position  $r$  were calculated using the following parabolic equations, according to the experimental results of previous studies [8–11].

$$u_r = a_u \left(\frac{r}{R}\right)^2 + b_u \quad (4)$$

$$N_r = a_N \left(\frac{r}{R}\right)^2 + b_N \quad (5)$$

where  $r$  is the radial distance from the center of the column,  $R$  the radius of the column,  $a_u$ ,  $b_u$ ,  $a_N$ , and  $b_N$  the numerical parameters in Eqs. (4) and (5). Previous experimental results indicated that the linear velocity of the mobile phase is 2–8% higher at the center of the column than near its wall and that the HETP is 80–150% higher near the wall than in the core of the column [1,8–11]. On the basis of these results, ratios  $u_w/u_c$  and  $N_w/N_c$  between 0.90 and 1.0, and between 0.2 and 1.0, respectively, were investigated. The subscripts  $w$  and  $c$  stand for the regions near the column wall and its center, respectively. However, the average flow velocity,  $u_{av}$ , of the mobile phase was adjusted so that the moment  $\mu_1$  of the overall peaks calculated remained equal to unity.  $u_{av}$  is calculated as follows.

$$u_{av} = \frac{\int_0^R 2\pi r u_r dr}{\pi R^2} \quad (6)$$

Substituting Eq. (4) into Eq. (6) gives  $u_{av}$  as  $(a_u/2) + b_u$ . At the same time,  $u_c = b_u$  and  $u_w = a_u + b_u$ . In this study, the values of  $a_u$  and  $b_u$  were adjusted so that  $u_{av} = 1$ . For example, in the case of  $u_w/u_c = 0.9$ ,  $a_u = -0.10526$  and  $b_u = 1.0526$ . On the other hand, the values of  $a_N$  and  $b_N$  were taken as  $-800$  and  $1000$ , respectively, when  $N_w/N_c = 0.2$  and  $N_c = 1000$ . The calculations of the peak profiles and its moments were made using a BASIC program.

### 3. Experimental

#### 3.1. Apparatus

A Shimadzu LC-6A high-performance liquid chromatograph was used. A small volume (a few  $\mu\text{l}$ ) of sample solution was introduced into the stream of mobile phase by use of a Rheodyne Model 7125 valve injector. A temperature-controlled water bath was used to maintain the column temperature constant. The eluent composition was monitored by the ultraviolet detector of the HPLC system.

#### 3.2. Columns and reagents

Two  $150 \times 6$ -mm YMC columns packed with  $45\text{-}\mu\text{m}$  spherical octadecylsilyl-silica gel were used. The carbon contents of the two packing materials were 8.6% (column 1) and 13.7% (column 2) (w/w). In order to reduce the influence of extra-column volumes on the tailing profile of the experimental peaks, columns packed with relatively large particles were used. The mobile phase was a methanol–water (70:30, v/v) solution. Water was prepared by distillation of ion-exchanged water. Sample components were benzene, ethylbenzene, *n*-butylbenzene, naphthalene, and anthracene. Uracil was used as the nonretained compound.

#### 3.3. Procedures

Chromatographic peaks were recorded under dif-

<sup>1</sup>Retention time of the peak maximum.

ferent sets of experimental conditions. Volumetric flow-rates of the mobile phase of 1 and 2 cm<sup>3</sup> min<sup>-1</sup> were used. The experiments were run at different temperatures in the range between 288 and 308 K. The parameters of the tailing peaks determined experimentally were the apical retention time, the peak widths at 10 and 50% of the peak height, and the asymmetry factor at the same heights. The asymmetry factor was defined as the ratio of the rear half-width of the elution peak,  $w_R$ , to the front half-width,  $w_F$ . The parameters were measured graphically. They characterize the tailing profiles.

#### 4. Results and discussion

##### 4.1. Influence of the radial heterogeneity of the flow velocity and the column efficiency on the peak tailing

Fig. 1 shows the peak profiles calculated under three different sets of conditions: (1)  $u_w/u_c=1.0$ ,  $N_w/N_c=1.0$ ; (2)  $u_w/u_c=0.95$ ,  $N_w/N_c=0.6$ ; and (3)  $u_w/u_c=0.9$ ,  $N_w/N_c=0.2$ . The importance of the radial variation of the mobile phase flow velocity and of the column efficiency increases in the order (1)<(2)<(3). In case (1), the peak profile is given by the

Gaussian distribution (Eq. (1)). The width of the calculated peaks increases with increasing degree of radial heterogeneity of the column. In case (3), the peak profile exhibits an obvious tailing. This result confirms that the radial heterogeneity of the flow velocity and the column efficiency are important causes of peak tailing.

Fig. 2 illustrates the influence of the radial variation of the flow velocity,  $u_w/u_c$ , on the apparent value of  $N$ . The ordinate is the ratio of  $N$  to the original value of  $N$  at the column center,  $N_c$ . The value of  $N$  was calculated from the moments  $\mu_1$  and  $\mu_2'$  of the elution peak. As explained above,  $\mu_1$  of all the peaks calculated is equal to unity. The value of the apparent second central moment,  $\mu_2'$ , was calculated by the following equation.

$$\mu_2' = \frac{\int_0^{\infty} C_d(t_d)(1-t_d)^2 dt_d}{\int_0^{\infty} C_d(t_d) dt_d} \quad (7)$$

where  $C_d(t_d)$  is the nondimensional concentration at  $t_d$ . The results shown in Fig. 2 indicate that band broadening increases with increasing degree of tail-

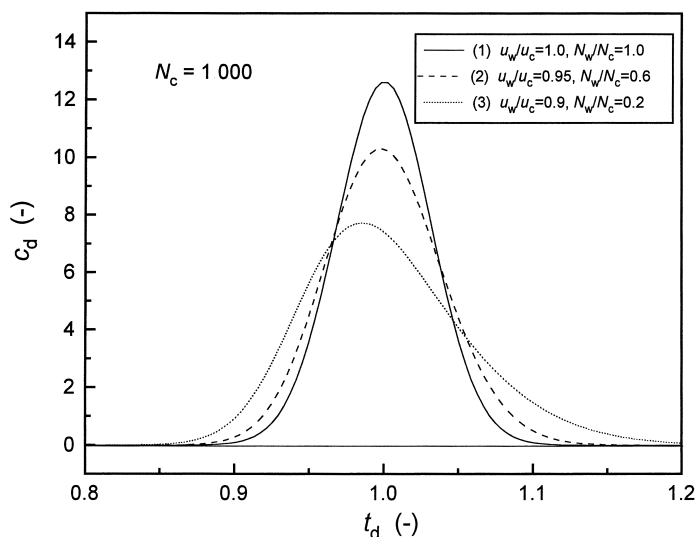


Fig. 1. Peak profiles calculated for three combinations of radial distributions of the mobile phase flow velocity and the column efficiency. Note that the symbol (-) used in all figures means that the parameter is dimensionless.

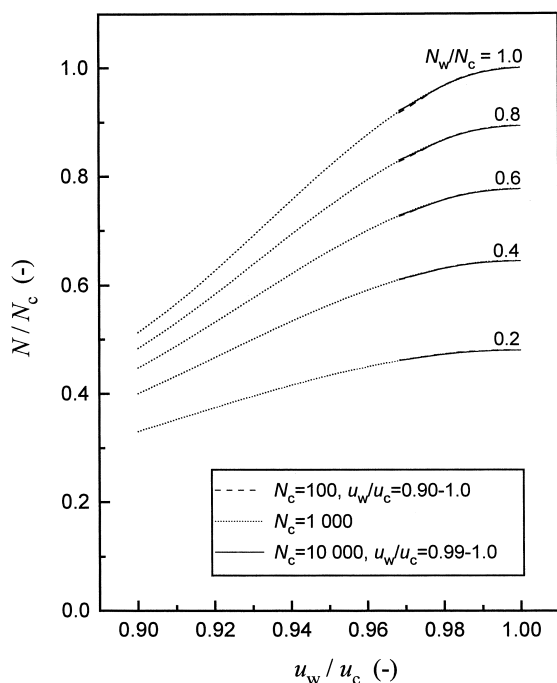


Fig. 2. Influence of the radial distributions of the mobile phase flow velocity and the column efficiency on the apparent efficiency. The column efficiency in the center region of the column is 1000 theoretical plates (dotted lines). The other two lines give the calculation results at  $N_c=100$ ,  $u_w/u_c=0.90-1.0$  (dashed lines) and at  $N_c=10\,000$ ,  $u_w/u_c=0.99-1.0$  (solid lines).

ing. The apparent value of  $\mu_2'$  is nearly three times larger when  $u_w/u_c=0.9$  and  $N_w/N_c=0.2$  than in the case of a Gaussian profile. Fig. 3 shows the correlation between the asymmetry factor of the elution peak at 10% peak height,  $(w_R/w_F)_{0.1}$ , and the relative importance of the change in the flow velocity,  $u_w/u_c$ . The degree of tailing of the peak increases with decreasing values of the ratios  $N_w/N_c$  and  $u_w/u_c$ . The value of  $(w_R/w_F)_{0.1}$  approaches 1.6 when  $u_w/u_c=0.9$  and  $N_w/N_c=0.2$ .

In Figs. 2 and 3, we show also the results of calculations performed at  $N_c=100$  and 10 000, with values of  $u_w/u_c$  between 0.90 and 1.0 and between 0.99 and 1.0, respectively. The lines calculated at  $N_c=100$  and 10 000 overlay exactly those corresponding to  $N_c=1000$ , indicating that the range of  $u_w/u_c$  between 0.968 and 1.0 at  $N_c=1000$  corresponds to the range between 0.90 and 1.0 at  $N_c=100$  and between 0.99 and 1.0 at  $N_c=10\,000$ . From the

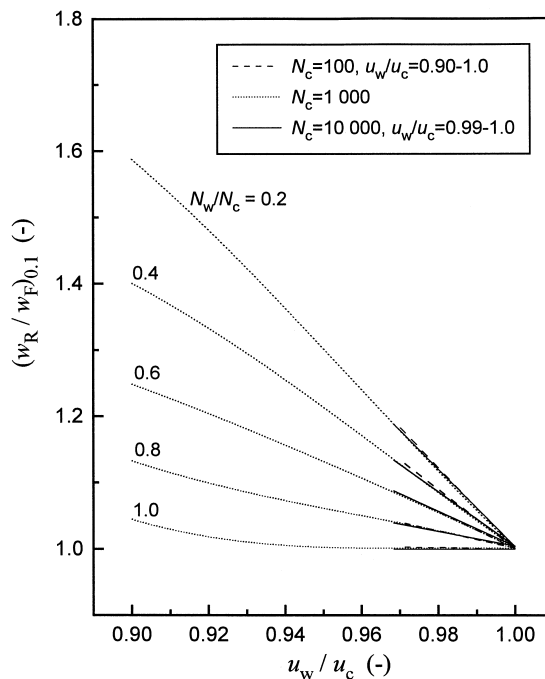


Fig. 3. Influence of the radial distributions of the mobile phase flow velocity and the column efficiency on the asymmetry factor of the elution peak. The column efficiency in the center region is 1000 theoretical plates (dotted lines). The dashed and solid lines correspond to the same values of the parameters as those in Fig. 2.

results in Figs. 2 and 3, it can be derived that columns having a high efficiency are more sensitive to a radial distribution of the flow velocity than low efficiency columns. This correlation can be represented by the following equation

$$\frac{1 - \left(\frac{u_w}{u_c}\right)_i}{1 - \left(\frac{u_w}{u_c}\right)_j} = \sqrt{\frac{N_j}{N_i}} \quad (8)$$

Eq. (8) suggests that the profiles of tailing peaks on columns of different efficiencies are similar if the values of  $N_w/N_c$  are the same, and that these profiles can be correlated. Thus, it may be possible to compare directly the amplitude of the radial distribution of the flow velocity in columns having different efficiencies. Therefore, all tailing peaks were calculated at  $N_c=1000$  in this study. In practice, chromatographic separations are carried out

with columns of different lengths, packed with materials of different size, run at different mobile phase flow velocities, and the retention of the sample components is different. Retention times and peak widths depend on the experimental conditions. However, a comparison between the characteristics of tailing peaks recorded under different conditions can be made by normalizing the values of the retention time and the peak width on the basis of the first moment of the tailing peaks.

The correlations shown in Figs. 2 and 3 suggest that new information on the degree of column radial heterogeneity can be derived from an analysis of the tailing peak profiles. Peak tailing can be characterized from various points of view. In this study, the following three characteristics were studied: (1) the decrease of the apical retention time; (2) the increase of the peak width; and (3) the extent of the asymmetry. The apical retention time,  $t_R$ , the peak width at 10 and 50% of the peak height,  $w_{0.1}$  and  $w_{0.5}$ , and the asymmetry factor at these heights,  $(w_R/w_F)_{0.1}$  and  $(w_R/w_F)_{0.5}$ , were derived for peaks calculated at  $N_c=1000$ . The correlations between some ratios of these parameters, e.g.,  $t_R/\mu_1$ ,  $w_{0.5}/w_{0.1}$ , and  $(w_R/w_F)_{0.1}$ , were calculated. Except for  $t_R/\mu_1$ , they probably provide results which are independent of  $N_c$  when tailing peaks on columns of different efficiency exhibit a similar shape.

#### 4.2. Retention times of tailing peaks

Fig. 4 illustrates the decrease of the apical retention time,  $t_R$ , which is due to a radial distribution of the flow velocity and the column efficiency. The ordinate is the ratio of  $t_R/\mu_1$ . In this study, the average flow velocity of the mobile phase was normalized in such a way that  $\mu_1$  was equal to unity for all the peaks calculated. The ratio  $t_R/\mu_1$  is plotted versus the asymmetry factor,  $(w_R/w_F)_{0.1}$  in Fig. 4. The value of  $t_R$  decreases with increasing degree of the peak tailing but the amplitude of the variation is small, the relative variation being approximately 1.5% under conditions such that  $(w_R/w_F)_{0.1}$  is close to 1.6. As illustrated in Fig. 2, the apparent value of  $N$  is reduced to about one third of  $N_c$  under such conditions. The results in Fig. 4 suggest that the retention time depends only on the degree of peak tailing. When the values of  $(w_R/w_F)_{0.1}$

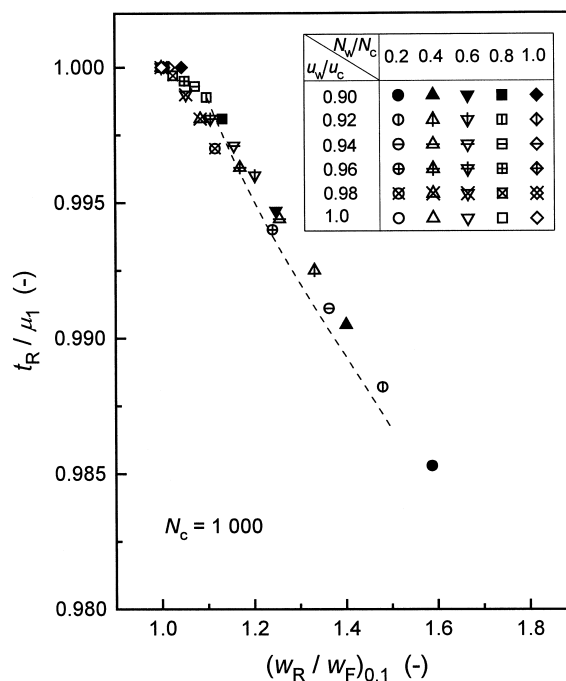


Fig. 4. Ratio of the apical retention time to the first moment of the elution peak as a function of the asymmetry factor at 10% of the maximum peak height. The column efficiency in the center region is 1000 theoretical plates. The symbols indicate the calculation results under various conditions of  $N_w/N_c$  and  $u_w/u_c$  (see matrix in legend). The dashed line represents the correlation calculated by the equations derived from the exponentially modified Gaussian (EMG) function by Foley and Dorsey [22].

$w_F)_{0.1}$  are same, almost the same value of  $t_R/\mu_1$  is obtained, even if the combination of the values of  $u_w/u_c$  and  $N_w/N_c$  is different. Because of the small amplitude of the variation of  $t_R$ , however, it is unlikely that some valuable information on the degree of column radial heterogeneity can be derived from a comparison between experimental data and the calculated results in Fig. 4.

Foley and Dorsey proposed an empirical equations for the calculation of chromatographic figures of merit for ideal and skewed peaks [22]. They analyzed the characteristics of tailing peaks having the exponentially modified Gaussian (EMG) function as a profile. This model was chosen arbitrarily, without any consideration of the mechanism of peak tailing. Some graphically measurable parameters of tailing elution peaks were correlated with the parameters of the EMG function. The dashed line in Fig. 4

illustrates the Foley–Dorsey correlation between  $t_R/\mu_1$  and  $(w_R/w_F)_{0.1}$ . A similar and parallel trend is observed between the dashed line and the plots calculated numerically in this study. However, the dashed line does not approach the point corresponding to the Gaussian peak at low values of  $(w_R/w_F)_{0.1}$ . Although some of the equations proposed by Foley and Dorsey are approximately correct for values of  $(w_R/w_F)_{0.1}$  larger than 1.09, they are not defined at lower values. The dashed line ends at  $(w_R/w_F)_{0.1} = 1.09$  although there are no reasons for that in this type of peak tailing.

#### 4.3. Width of tailing peak

When a chromatographic peak exhibits tailing, its width at low concentrations is larger than at high ones. The ratio of the peak widths at different fractional heights may be one of the characteristics of the tailing peak. Fig. 5 illustrates the correlation between  $w_{0.5}/w_{0.1}$  and  $(w_R/w_F)_{0.1}$ . In contrast to Fig. 4, the data points are scattered in a wide range. The ratio  $w_{0.5}/w_{0.1}$  should be equal to 0.549 when the peak profile is Gaussian. The value of  $w_{0.5}/w_{0.1}$  depends on the nature of the radial heterogeneity of the column. For equal values of  $(w_R/w_F)_{0.1}$ , different values of  $w_{0.5}/w_{0.1}$  are observed for different combinations of the values of  $u_w/u_c$  and  $N_w/N_c$ . The results in Fig. 5 suggest that values of  $w_{0.5}/w_{0.1}$  higher than 0.549 may be observed for tailing peaks under some conditions. However, these conditions may be unrealistic. As shown in Fig. 6, the experimental data (symbols  $\circ$  and  $\triangle$ ) are found only in a limited region of the graph, between the two solid lines in Fig. 6, indicating that  $w_{0.5}/w_{0.1}$  decreases from the limit point corresponding to a Gaussian profile with increasing  $(w_R/w_F)_{0.1}$ . The network of dotted lines in Fig. 6 illustrates the calculation results shown in Fig. 5. The results in Figs. 5 and 6 provide some information on the radial heterogeneity of the column, i.e., on the correlation between  $u_w/u_c$  and  $N_w/N_c$ .

Figs. 5 and 6 also illustrate the correlation between  $w_{0.5}/w_{0.1}$  and  $(w_R/w_F)_{0.1}$  calculated from the equations proposed by Foley and Dorsey [22] (dashed line). This dashed line is mainly located in the region between the two solid lines in Fig. 6. However, it can account for the peak tailing charac-

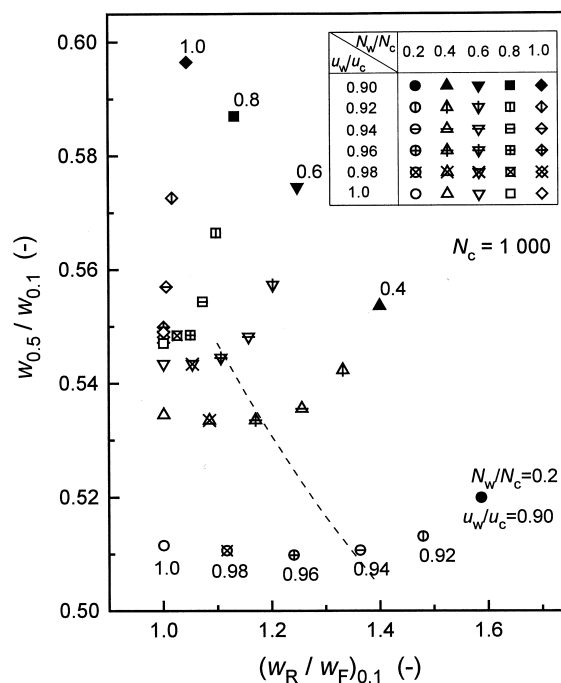


Fig. 5. Correlation of the peak widths at 10 and 50% of the maximum peak height with the asymmetry factor at 10% of the peak height. The column efficiency in the center region is 1000 theoretical plates. The symbols indicate the calculation results under various conditions of  $N_w/N_c$  and  $u_w/u_c$  (see matrix in legend). They are same combinations as those used in Fig. 4. The dashed line represents the correlation calculated by the equations derived from the EMG function.

teristics only under extremely limiting conditions. Even if we limit ourselves to the sources of peak asymmetry arising from a heterogeneous column bed, we find that there are many types of tailing profiles, the characteristics of which cannot be interpreted by the empirical equations derived from the EMG function. Note that it is also unreasonable that the dashed line does not pass even close to the point  $(w_R/w_F)_{0.1} = 1.0$  and  $w_{0.5}/w_{0.1} = 0.549$ .

#### 4.4. Correlation between $u_w/u_c$ and $N_w/N_c$

Fig. 7 illustrates the correlation between  $u_w/u_c$  and  $N_w/N_c$  derived from the results in Figs. 5 and 6. The two solid lines in Fig. 7 correspond to those in Fig. 6, between which are found the experimental results. The influence of the amplitude of the radial distribution of the local column efficiency is am-

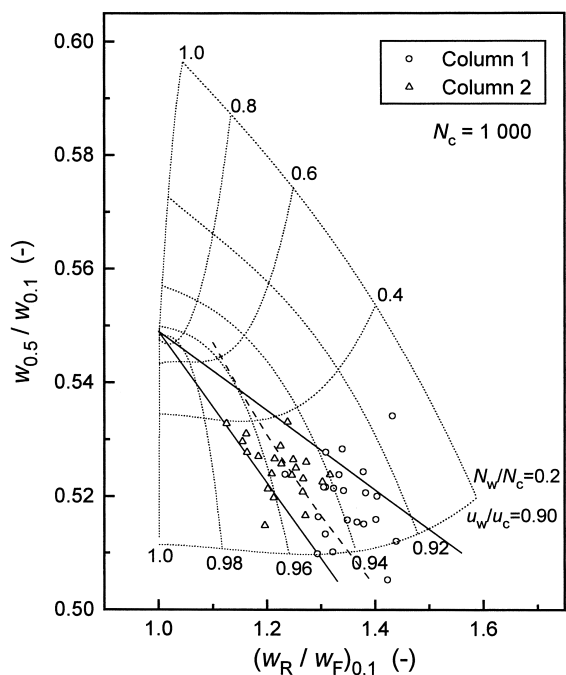


Fig. 6. Correlation of the peak widths at 10 and 50% of the maximum peak height with the asymmetry factor at 10% of the peak height. The experimental data are represented by the symbols ( $\circ$ ) for column 1 and ( $\triangle$ ) for column 2. The dashed line represents the correlation calculated by the equations derived from the EMG function. The dotted lines are the same as those connecting the symbols in Fig. 5. They represent the results of the theoretical calculations.

plified by an increase in the amplitude of the flow velocity distribution. The results in Fig. 7 indicate that no experimental data were ever observed in regions in which the radial heterogeneity of the column bed affects only either the flow velocity distribution or that of the column efficiency. For example, a variation of the flow velocity in the radial irregularity is always the result of a heterogeneous bed which causes also a radial variation of the local column efficiency.

Experimental data on the radial distributions of the flow velocity and the column efficiency have been reported for columns having different efficiencies [5,6,8–11]. However, it is difficult directly to compare these experimental data, the columns having different efficiencies. In this study, the values of

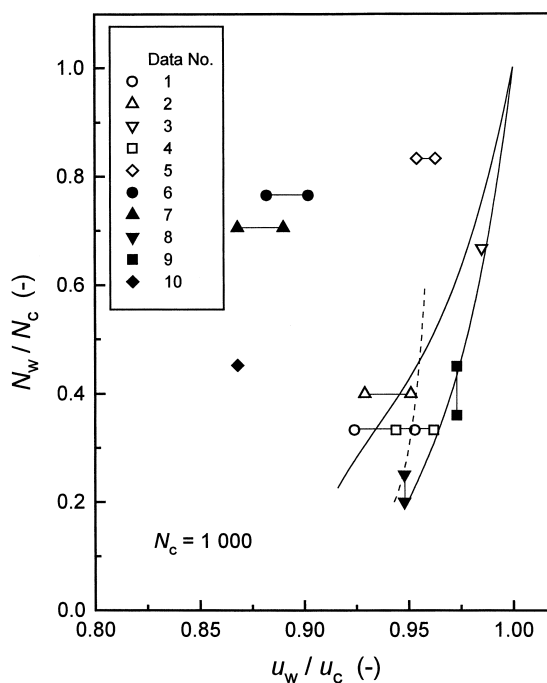


Fig. 7. Correlation of the radial distributions of the mobile phase flow velocity and the column efficiency. The column efficiency in the center region is 1000 theoretical plates. Data numbers refer to Table 1. The dashed line represents the correlation calculated by the equations derived from the EMG function.

$u_w/u_c$  determined experimentally and corresponding to a certain value of  $N_c$  were converted to values corresponding to  $N_c = 1000$  by applying Eq. (8). The results are reported in Table 1. Fig. 7 also shows the experimental data. These are given as plots of  $N_w/N_c$  versus the converted amplitude of the flow velocity distribution,  $u_w/u_c(1000)$ . Most data points are located in the region between or around the two solid lines. Although a few data scatter farther, they also support the existence of a correlation between  $N_w/N_c$  and  $u_w/u_c$ . The scatter of the data points results probably from experimental errors made in the determination of  $u_w/u_c$ . The relatively high values of  $N_c$  in the experiments referred as #5, 6, 7 and 10 causes an amplification of the error when the values of  $u_w/u_c$  are converted. Nevertheless, the results shown in Figs. 5–7 indicate that the amplitude of the radial distributions of the flow velocity and the column efficiency can be estimated by a proper



Table 1  
Experimental data on the radial distributions of the mobile phase flow velocity and the local column efficiency

Column	Packing materials		Efficiency			Radial heterogeneity			Data	Ref.
	$d_p^a$ ( $\mu\text{m}$ )	Size (mm)	$h_c^b$	$h_w^c$	$N_c^d$	$N_w/N_c^e$	$u_w/u_c(N_c)^f$	$u_w/u_c(1000)^g$		
Glass beads	40	200×4.6	5.5	16.5	900	0.33	0.92–0.95	0.92–0.95	1	[8]
Porous silica	10	200×4.6	10	25	2000	0.4	0.95–0.965	0.93–0.95	2	[8]
Zorbax C <sub>18</sub>	10	100×4.6	10	15	1500	0.67	0.988	0.985	3	[9]
Zorbax C <sub>18</sub>	10	300×7.8	6	18	5000	0.33	0.975–0.983	0.94–0.96	4	[10]
Zorbax C <sub>8</sub>	5	250×9.4	5.4	6.5	9300	0.83	0.985–0.988	0.95–0.96	5	[10]
Zorbax C <sub>18</sub>	10	150×50	3.9	5.1	3900	0.77	0.94–0.95	0.88–0.90	6	[11]
Zorbax C <sub>18</sub>	10	150×50	3.1	4.4	4800	0.71	0.94–0.95	0.87–0.89	7	[11]
RP-18	3	100×3.2	5	20–25	6700	0.20–0.25	0.98	0.95	8	[5]
RP-18	3	100×3.2	4.5	10–12	7400	0.36–0.45	0.99	0.97	9	[5]
RP-18	3	40×3.2	1.9	4.2	7000	0.45	0.95	0.87	10	[6]

<sup>a</sup>Particle diameter.

<sup>b</sup>Reduced HETP at the center of the column.

<sup>c</sup>Reduced HETP near the wall of the column.

<sup>d</sup>Number of theoretical plates at the center of the column.

<sup>e</sup>Ratio of the column efficiency near the wall to that at the center of the column.

<sup>f</sup>Ratio of the flow velocity near the wall to that at the center of the column under the conditions that the column efficiency is equal to  $N_c$ .

<sup>g</sup>Conversion ratio of the flow velocity near the wall to that at the center of the column under the conditions that the column efficiency is equal to 1000.

analysis of the information available in the peak width and the asymmetry of the overall elution peak.

The dashed line in Fig. 7 shows the correlation between  $N_w/N_c$  and  $u_w/u_c$  calculated using the equations proposed by Foley and Dorsey [22]. The results in Figs. 5–7 suggest that the EMG function cannot provide a comprehensive representation of tailing profiles in chromatographic peaks arising from column bed heterogeneity.

#### 4.5. Asymmetry of tailing peaks

Like the radial variation of the peak width, the cross-sectional variation of the asymmetry at different peak heights may serve to characterize the tailing of peaks. Fig. 8 illustrates the correlation between  $(w_R/w_F)_{0.5}$  and  $(w_R/w_F)_{0.1}$ . A significant scatter of the plot is observed. It is unlikely that information about the column radial heterogeneity can be derived from a comparison between the results of calculations and the experimental data. The results in Fig. 8 mainly show that  $(w_R/w_F)_{0.1}$  is larger than  $(w_R/w_F)_{0.5}$  when chromatographic peaks exhibit tailing profiles. The correlation based on the EMG function

(dashed line) shows again a trend which is different from that of the graphs calculated in this study.

## 5. Conclusions

The radial heterogeneity of the column bed is an important contribution to peak tailing in analytical chromatography. The higher the column efficiency, the larger the effect of a given degree of radial heterogeneity on the extent of peak tailing. Eq. (8) allows a correlation between the amplitude of the radial variation of the flow velocity for columns having different efficiencies. The value of  $t_R/\mu_1$  decreases with increasing asymmetry factor,  $(w_R/w_F)_{0.1}$  and depends only on the degree of peak tailing. However, the magnitude of the variation is small. By contrast, the ratio  $w_{0.5}/w_{0.1}$  depends on the nature of the radial heterogeneity of the column. Plots of calculated values of  $w_{0.5}/w_{0.1}$  against  $(w_R/w_F)_{0.1}$  are widely scattered. A comparison of the experimental data and the calculation results of this study provided, however, curved correlations between  $u_w/u_c$  and  $N_w/N_c$  which show that  $N_w/N_c$  increases with increasing  $u_w/u_c$ .

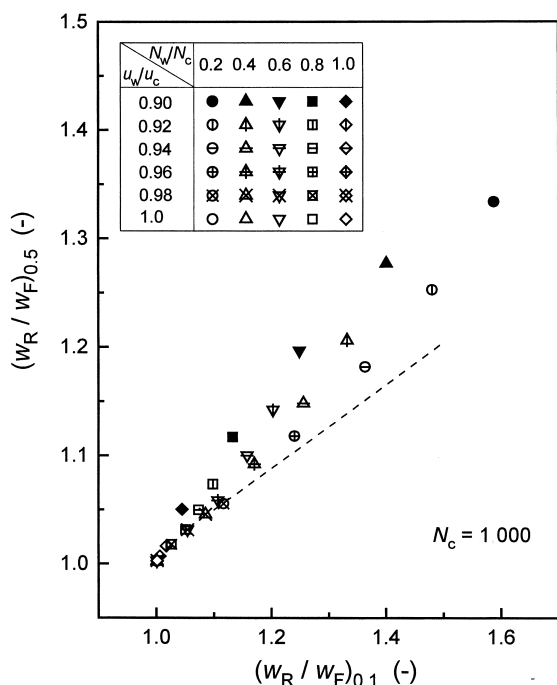


Fig. 8. Correlation between the asymmetry factors at 10 and 50% of the peak height. The column efficiency in the center region is 1000 theoretical plates. The symbols indicate the calculation results under various conditions of  $N_w/N_c$  and  $u_w/u_c$  (see matrix in legend) and are the same as those in Fig. 4. The dashed line represents the correlation calculated by the equations derived from the EMG function.

Previous experimental data relating to the radial variation of the mobile phase flow velocity and the column efficiency could be plotted on these correlations, suggesting that experimental data on column radial heterogeneity measured on columns having different efficiencies could be directly compared. The magnitude of the radial heterogeneities of the flow velocity and the column efficiency could be evaluated by analyzing the peak width and the asymmetry factor of the elution peak. Plots of  $(w_R/w_F)_{0.5}$  against  $(w_R/w_F)_{0.1}$  indicated that  $(w_R/w_F)_{0.1}$  was larger than  $(w_R/w_F)_{0.5}$  for chromatographic peaks exhibiting tailing profiles. Finally, the empirical equations derived from the EMG function do not properly characterize tailing peaks originating from bed heterogeneity.

## 6. Symbols

$a_N$	Coefficient in Eq. (5)
$a_u$	Coefficient in Eq. (4)
$A_p$	Area of the injected pulse
$b_N$	Coefficient in Eq. (5)
$b_u$	Coefficient in Eq. (4)
$C$	Actual solute concentration
$C_d$	Dimensionless concentration
$d_p$	Particle diameter
$h$	Reduced HETP
$k'_0$	Retention factor at infinite dilution
$L$	Column length
$n$	Amount of the solute injected
$N$	Number of theoretical plates
$N_r$	Number of theoretical plates at a radial position $r$
$r$	Radial distance from the center of the column
$R$	Column radius
$S$	Column cross-sectional area
$t$	Time
$t_d$	Dimensionless time
$t_R$	Retention time
$u$	Interstitial velocity of the mobile phase
$u_{av}$	Average mobile phase flow velocity
$u_r$	Linear velocity at a radial position $r$
$w$	Peak width
$w_F$	Front half-width of the elution peak
$w_R$	Rear half-width of the elution peak
$w_R/w_F$	Asymmetry factor

### 6.1. Greeks

$\epsilon$	Total porosity of the column
$\mu_1$	First moment
$\mu'_2$	Second central moment
$\sigma_d$	Dimensionless standard deviation

### 6.2. Subscripts

$c$	At the center of the column
$i$	$i$ th column
$j$	$j$ th column
$w$	Near the wall of the column
0.1	At 10% of maximum peak height
0.5	At 50% of maximum peak height

## Acknowledgements

This work was supported in part by Grant CHE-97-01680 of the National Science Foundation and by the cooperative agreement between the University of Tennessee and the Oak Ridge National Laboratory. We acknowledge the support of Maureen S. Smith in solving our computational problems.

## References

- [1] G. Guiochon, T. Farkas, H. Guan-Sajonz, J.-H. Koh, M. Sarker, B.J. Stanley, T. Yun, *J. Chromatogr. A* 762 (1997) 83.
- [2] D.S. Horne, J.H. Knox, L. McLaren, *Sep. Sci.* 1 (1966) 531.
- [3] J.H. Knox, G.L. Laird, P.A. Raven, *J. Chromatogr.* 122 (1976) 129.
- [4] C.H. Eon, *J. Chromatogr.* 149 (1978) 29.
- [5] J.E. Baur, E.W. Kristensen, R.M. Wightman, *Anal. Chem.* 60 (1988) 2334.
- [6] J.E. Baur, R.M. Wightman, *J. Chromatogr.* 482 (1989) 65.
- [7] J.H. Knox, J.F. Parcher, *Anal. Chem.* 41 (1969) 1599.
- [8] T. Farkas, J.Q. Chambers, G. Guiochon, *J. Chromatogr. A* 679 (1994) 231.
- [9] T. Farkas, M.J. Sepaniak, G. Guiochon, *J. Chromatogr. A* 740 (1996) 169.
- [10] T. Farkas, G. Guiochon, *Anal. Chem.* 69 (1997) 4592.
- [11] T. Farkas, M.J. Sepaniak, G. Guiochon, *AIChE J.* 43 (1997) 1964.
- [12] U. Tallarek, E. Baumeister, K. Albert, E. Bayer, G. Guiochon, *J. Chromatogr. A* 696 (1995) 1.
- [13] E. Bayer, E. Baumeister, U. Tallarek, K. Albert, G. Guiochon, *J. Chromatogr. A* 704 (1995) 37.
- [14] U. Tallarek, E. Bayer, G. Guiochon, *J. Am. Chem. Soc.* 120 (1998) 1494.
- [15] T. Yun, G. Guiochon, *J. Chromatogr. A* 760 (1997) 17.
- [16] T. Yun, G. Guiochon, *J. Chromatogr. A* 672 (1994) 1.
- [17] T. Yun, G. Guiochon, *J. Chromatogr. A* 734 (1996) 97.
- [18] G. Guiochon, S. Golshan-Shirazi, A.M. Katti, *Fundamentals of Preparative and Nonlinear Chromatography*, Academic Press, Boston, MA, 1994.
- [19] T. Fornstedt, G. Zhong, G. Guiochon, *J. Chromatogr. A* 741 (1996) 1.
- [20] T. Fornstedt, G. Zhong, G. Guiochon, *J. Chromatogr. A* 742 (1996) 55.
- [21] K. Miyabe, G. Guiochon, *J. Chromatogr. A* (in press).
- [22] J.P. Foley, J.G. Dorsey, *Anal. Chem.* 55 (1983) 730.